JOURNAL OF CHEMICAL INFORMATION AND MODELING

Article

pubs.acs.org/jcim

Electron Density Distribution in Endohedral Complexes of Fullerene C_{60}, Calculated Based on the Gauss Law

Nina Sadlej-Sosnowska*[,†] and Aleksander P. Mazurek[†,‡]

[†]National Medicines Institute, 30/34 Chełmska Street, 00-725 Warsaw, Poland

[‡]Department of Drug Chemistry, Medical University of Warsaw, 1 Banach Street, 02-097 Warsaw, Poland

ABSTRACT: This study demonstrates that different partial charge methodologies, consisting of an attribution of the total electron density to particular atoms of a molecule, generate very divergent results in the case of atoms doped into a fullerene cage. A new method of calculating the density distribution inside and outside fullerene complexes has been proposed and applied in the case of C_{60}, $[F@C_{60}]^-$, $[Na@C_{60}]^+$, and $He@C_{60}$. It allowed for the calculation of the electron density between surfaces, isomorphic with the C_{60} cage, lying inside and outside the latter, as well as the charge in the space surrounding the central atom (or the central point in the case of empty C_{60}).

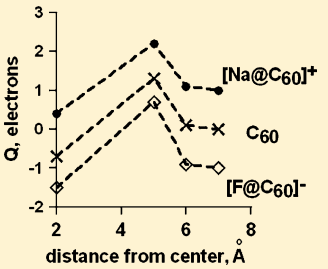

INTRODUCTION

One of the most exciting features of C_{60} and higher fullerenes is that their carbon cages have inner cavities large enough to hold an atom or even small molecules. Stable compounds of He and Ne and other noble gases[1−4] N[5,6] as well as alkali group 2 and rare-earth metals[7,8] have been synthesized, as well as fullerenes with H_2,[9,10] H_2O,[11] CO, and N_2.[3]

In the case of the neutral atoms/molecules such as He, N, and H_2, the dopant is placed in the center of the cage;[4−6] the results have been proven by theoretical methods.[12] In the case of alkali metals, endo- and exo- complexation takes place.[13] In metal endohedral fullerenes, the metal is generally located at an off-center position inside the cage.[4,7,14] Of the plethora of theoretical papers dealing with the structural, thermodynamic, and electronic properties of doped fullerenes, we mention here a study that appeared only recently, where the stability of various anions (F^-, Cl^-, Br^-, OH^-, and CN^-) in fullerenes of various sizes (C_{30}−C_{70}) was investigated.[15]

The electron population associated with a given atom in a molecule is of considerable interest with regard to the chemical properties and reactivity; the same is true for atoms and molecules that are components of a complex. In papers devoted to endohedrally doped fullerenes, one question is frequently raised: What is the distribution of the overall charge between the cage and the dopant? One source of this information on the electronic structure, properties, and charges in complexes is based on the calculated or measured physicochemical properties of the complexes. In the case of Li as a dopant, full electron transfer to the cage has been found on the basis of calculated spin density.[16] In the case of the fullerene doped with small hydrocarbons, a small quantity of electron transfer from C_{60} to the hydrocarbon molecule (C_2H_2, C_2H_4, and C_2H_6) was found on the basis of the calculated NMR shifts; the NMR signals of the carbon atoms from the hexagon were shifted to a slightly lower field when the incorporation occurred.[17] For metallofullerenes, on the basis of various spectrometric methods, such as EPR, NMR, UV−vis, and XPS, it is generally accepted that three-electron transfer is favorable when M = Y, La, Ce, Pr, Nd, Gd, Tb, Dy, Ho, Er, or Lu, but Sc, Eu, Sm, Yb, Tm, Ca, Sr, and Ba prefer to donate two electrons to the fullerene cages.[8]

For calculating the charges of the components of a complex (similar to evaluating charges of atoms in a molecule), there is a need to attribute the overall electron population to the particular atoms of the dopants and of the cage. Because the calculation of atomic charges relies upon some arbitrary partitioning of the electron density to individual atoms, the results generated by different algorithms can vary considerably. In studies where a theoretical method of electron density partitioning has been applied, the results obtained by one method have most frequently been reported. For example, Mulliken population analysis of a fullerene with an encapsulated water molecule showed polarization of the cage, but not a net charge transfer between the cage and the H_2O molecule.[18] A similar result was obtained for $N@C_{60}$: Mulliken population analysis showed that essentially no charge transfer between N and C_{60} occurred (Mulliken population at N was 6.982 e).[19]

Generalized Atomic Polar Tensor (GAPT) charges (calculated from the computed nuclear derivatives of dipole moments) pointed to negative dopant charges in the cases of $H_2@C_{60}$, $N_2@C_{60}$, $CO@C_{60}$, $HF@C_{60}$, $LiH@C_{60}$, and $LiF@C_{60}$.[20] Therefore, in all cases, the fullerene acts as a weak electron donor.

The charges of dopants were also calculated using Natural Population Analysis (NPA charges). In a series of endohedral complexes with noble gas atoms, charges of 0.0, 0.01, 0.01, 0.03, and 0.53 were found for He, Ne, Ar, Kr, and Xe, respectively.[21] The results of both Mulliken and NPA population analysis schemes of the charge transfer in the neutral and charged $Li@C_{60}$ complexes with total charges ranging from +3 to −1 were interpreted as showing that the fullerene acts as an electron

Received: January 2, 2012
Published: April 27, 2012

buffer, with the Li charge remaining +1 regardless of the total charge and geometry (Li in the cage center or off-center).[22]

Apart from the calculations of charge transfer in Li@C_{60} carrying a total charge of −1, we have not found any other results with respect to the negatively charged complexes. Therefore, we calculated the charges of the fluorine atom and the cage, in the case of a simple complex, as being negatively charged F@C_{60}. Taking into account that there is no universally agreed upon "best" procedure for computing a partial atomic charge,[23] the charges obtained by seven different algorithms were compared. The results were different to a such degree (shown in the Results section) that we undertook the task of calculating the distribution of electron density in a few fullerenes on the basis of a different principle.

Our calculation of the distribution of electric charge is based on the application of the Gauss law, which states that the charge in a region of space can be deduced by integrating the electric field through a closed surface comprising the charge in order to find the flux of the electric field; the flux through any closed surface is proportional to the electric charge inside it[24]

$$\Phi_{E,S} = \oint E\cdot \mathrm{d}S = 4\pi Q = 4\pi \sum_i q_i = 4\pi \oint \rho \mathrm{d}\nu \quad (1)$$

In the equation, $\Phi_{E,S}$ denotes the flux of the electric field E through the surface S, ρ is the electron density within a volume $\mathrm{d}\nu$, $\oint E\cdot \mathrm{d}S$ is a surface integral, and the last three terms represent the total charge enclosed by S, multiplied by 4π.

THEORETICAL METHODS

The calculations were performed using the DFT functional MPWB1K.[25,26] For the calculations, the Gaussian G09 package (revision B.01) was employed.[27] In view of the relatively large size of the systems included in this study, we selected the 3-21+G basis set[28] for the geometry optimizations. We started with the calculations of the fluorine charge inside the optimized, negatively charged F@C_{60}. Seven different algorithms for partitioning the total electron density between C and F atoms were used: Mulliken,[29] NPA,[30] Löwdin,[31] AIM,[32] and Hirshfeld,[33] and those based on fitting charges to the electrostatic potential (CHelpG[34] and Merz−Singh−Kollman schemes).[35] The charges based on the Atoms in Molecules Theory[32] were calculated by the AIM2000 program.[36]

The calculated charges were significantly different (Table 1 in the Results section), similar to when the charges were calculated for positively charged Na@C_{60} (Table 2). Therefore, we sought another way of estimating the charges and applied a method based on the Gauss law.

In order to find the charge originating from an object (ion or atom) placed at the center of a fullerene cage, as well as of the cage itself, we had to calculate the electric flux through a surface enclosing the object. We selected surfaces similar to the surface of the cage and concentric to it but reduced or enlarged. Each surface was comprised of 20 hexagons and 12 pentagons, thus resembling the C_{60} cage. Calculations of the flux over the different surfaces allowed us to find the charge enclosed in a smaller or larger volume around the center of the complex, point O. The electric field was calculated at the MPWB1K/3-21+G and MPWB1K/6-31+G*//MPWB1K/3-21+G levels, as well as at the MP2/3-21+G//MPWB1K/3-21+G and MP2/6-31+G*//MPWB1K/3-21+G levels in order to see how utilizing the MP2 electron density instead of the DFT one can affect the results of this paper.

For the reduced surface, the distance d_h between the centers of the hexagons and O was set to 2 Å; for the enlarged surfaces, this was set to 5, 6, 7, and 10 Å. Values of d_p were slightly larger than d_h; this meant that the pentagon centers were more distant from O than were the hexagon centers. For example, on the smallest surface, the corresponding distances were 2.0442 Å (pentagons) and 2 Å (hexagons). The values of d_h and d_p were the closest distances between the center of the fullerene and the six- and five-membered rings of the traced surfaces.

The first (reduced surface) contained an ion or atom doped into the cage or nothing (in the case of empty C_{60}). The remaining surfaces comprised the entire fullerene cage with (or without) a dopant inside. To obtain the coordinates of the vertices of the reduced/enlarged surfaces, the Cartesian coordinates of all C atoms of the cage were scaled in the same proportion.

The next step was to calculate the values of the electric field passing through the centers of the scaled hexagons and pentagons. The symmetry of the system mandated that $E_6(0)$, the electric field passing through the center of each hexagon, was the same; this also holds for $E_5(0)$, the electric field passing through the centers of the pentagons. The directions of both $E_6(0)$ and $E_5(0)$ are in line to normal to the surface of each polygon.

However, the electric field passing through different points of a hexagon (E_6) or pentagon (E_5) is not equal to $E_6(0)$ or $E_5(0)$ nor is it perpendicular to the surface normal. Therefore, for a given surface, a straight line was traced between the center and a vertex of a hexagon (or pentagon), and the electric field was calculated at nine intermediate points lying on it and at the vertex. To find these points, we used the parametric equations of a straight line in a three-dimensional space, passing through a (x_0, y_0, z_0) point and parallel to an [**a**, **b**, **c**] vector[37]

$$x = x_0 + \mathbf{a}t$$

$$y = y_0 + \mathbf{b}t$$

$$z = z_0 + \mathbf{c}t$$

Here, the (x_0, y_0, z_0) point is the center of a hexagon or pentagon and vector components **a**, **b**, **c**, equal $x_v - x_0$, $y_v - y_0$, and $z_v - z_0$, where x_v, y_v, and z_v are the coordinates of a corresponding vertex. Subsequently, the field was calculated at 10 points on the line, corresponding to t = 0.1, 0.2,.....,0.9, 1.0. A graph of E as a function of distance from the polygon center for two surfaces, reduced ("2A") and first enlarged ("5A"), can be found in Figure 1. In the Figure, the extreme left points correspond to polygon centers, whereas the extreme right correspond to vertices and have the same ordinate value for the hexagon and pentagon belonging to the same surface.

The calculated values of the electric field are necessary but insufficient to obtain the flux of the electric field through the surface of hexagon/pentagon because E at all points but the polygon center is not perpendicular to the polygon surface; therefore, we have to calculate the projection of E onto the normal to the surface. To do this, we took advantage of the scalar product of two vectors: one normal to the polygon surface and passing through its center and the $[E_x, E_y, E_z]$ vector at a given point. Division of the scalar product by the length of the normal vector produced the length of the projection of E on it, E_n. With the E_n values calculated, their functional dependence on the distance from the polygon center could be found by means of polynomial fitting (of the second

dx.doi.org/10.1021/ci300001h | J. Chem. Inf. Model. 2012, 52, 1193−1198

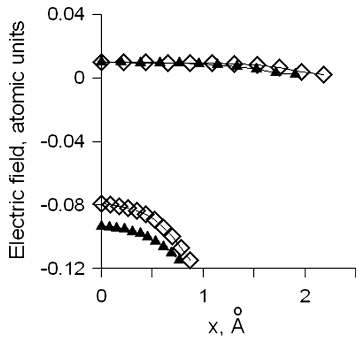

Figure 1. Diminution of the electric field going from a polygon center (◊ - hexagons, E_6, ▲- pentagons, E_5) toward a vertex of the icosahedral surface in $[F@C_{60}]^-$. x is the distance from the polygon center to the vertex.

order). Thus, one thing remained to be done, namely, the calculation of the surface integral $\oint E \cdot dS$. In order to simplify the calculation, the hexagon/pentagon surface was replaced by a circle of the same area, with a radius denoted as R. The equation fitting the (x, E_n) points, where x is the distance of a given point to the polygon center, was a polynomial of the second order, $A + Bx + Cx^2$. In this case, integration of E through S resulted in

$$\oint E \cdot dS = \int_0^R 2\pi x(A + Bx + Cx^2)dx$$
$$= 2\pi(A \times R^2/2 + B \times R^3/3 + C \times R^4/4) \quad (2)$$

The flux through 20 hexagons was added to the flux through 12 pentagons to produce the total flux over the entire closed surface, $\Phi_{E,S}$, and the total enclosed charge Q was calculated from eq 1.

Units. The electric field calculated by the Gaussian program is given in atomic units (au). One au of E equals 5.1422×10^{11} V/m.[38] Taking into account the following: [39]

> 1 V = 1/299.8 esv, where esv is an electrostatic unit of voltage,
> esv = esu/cm, where esu is the charge in electrostatic units,
> $e = 4.803 \times 10^{-10}$ esu, where e is the charge of an electron, an atomic unit of charge,

we obtain:

one au of $E = 3.571 \times 10^{16}$ e/cm^2. Then, the product of an electric field of 1 au and a surface of $(1$ Å$)^2$ equals 3.571 e.

RESULTS

The results of calculating the charge on an F atom in $[F@C_{60}]^-$, with the application of seven of known schemes of partitioning electron density to individual atoms, are shown in Table 1.

The results of the first six algorithms agreed in that the density of the additional electron was distributed between the F atom and the cage. However, the amount assigned to the both fragments differed significantly. The results based on fitting the charges to electrostatic potential (according to the MK scheme) were unphysical.

We checked if similar discrepancies would be obtained for the Na charge in $[Na@C_{60}]^+$. The results of the application of seven of known schemes of partitioning an electron density in $[Na@C_{60}]^+$ to individual atoms are shown in Table 2.

Table 1. Charge on F Atom inside $[F@C_{60}]^-$ Calculated with the MPWB1K Functional Using Seven Different Algorithms

	Basis set	
Scheme	3-21+G	6-31+G*
Mulliken	−0.83	−0.76
NPA	−0.79	–
Löwdin	−0.62	−0.64
Hirshfeld	−0.58	−0.54
AIM	−0.86	−0.92
CHelpG	−0.06	−0.03
MK	17.73	13.82

Table 2. Charge on an Na Atom inside $[Na@C_{60}]^+$, Calculated with the MPWB1K Functional Using Seven Different Algorithms

	Basis set	
Scheme	3-21+G	6-31+G*
Mulliken	11.91	3.15
NPA	1.75	–
Löwdin	0.86	0.79
Hirshfeld	0.41	0.47
AIM	0.00	0.03
CHelpG	0.65	0.65
MK	10.16	5.27

The results shown in Table 2 are even more scattered than those for F in $[F@C_{60}]^-$. According to four schemes (Löwdin, Hirshfeld, AIM, and CHelpG), the result can be interpreted as a transfer of some electron density from the C_{60} cage to the Na^+ ion inside. Three methods anticipate the transfer of electron density from the ion to the cage, even so large as over three to five electrons with the 6-31+G* basis set. There is no reason to believe the outcome of any particular algorithm.

Keeping this in mind, we calculated the charges by applying an entirely different philosophy. Instead of ascribing charges to particular atoms, the space distribution of the electric charge inside and outside the cage was determined; on this basis, one might infer what charge may be attributed to an atom positioned inside the cage. In addition to the negatively charged $[F@C_{60}]^-$, calculations were also performed for empty C_{60}, positively charged $[Na@C_{60}]^+$, and neutral $He@C_{60}$ and were based on application of eq 1.

We checked that the electric field inside and outside the C_{60} cage displayed the same symmetry Ih as the cage itself; namely, the $E_6(0)$ values on each added surface in the direction perpendicular to O and passing through the hexagons centers were the same. It also held for $E_5(0)$, the electric field passing through the centers of the pentagons. The direction of both $E_6(0)$ and $E_5(0)$ were in line to the normal to the surface of each hexagon or pentagon. The dependence of $E_6(0)$ on the distance from the global center, O, is shown in the left panel of Figure 2.

Calculation of E and Q, according to eq 1, was completed by the simultaneous determination of the signs of E and Q, on the basis of the known components E_x, E_y, and E_z of E. The calculated charges (in au) enclosed within the icosahedral surfaces similar to the C_{60} surface, of successively increasing volume, are shown in Table 3, as well as their comparison for the four investigated compounds.

dx.doi.org/10.1021/ci300001h | J. Chem. Inf. Model. 2012, 52, 1193−1198

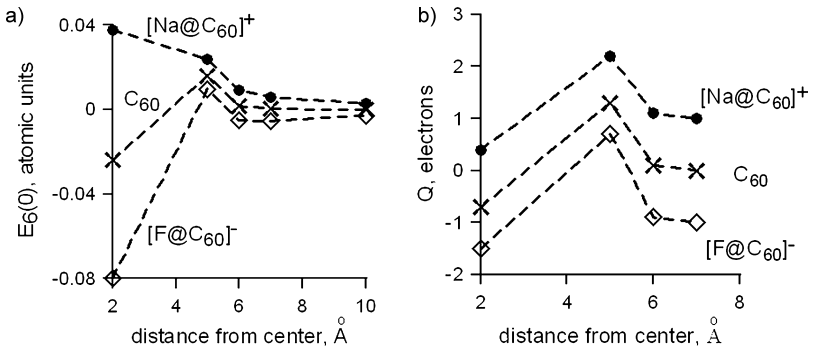

Figure 2. (Left) Dependence of the electric field $E_6(0)$ at hexagon centers on the distance of the centers from the complex center, O. (Right) The points represent charges Q enclosed within the icosahedral surfaces isomorphic with the C_{60} cage, characterized by the distance of hexagons centers from the complex center O by 2, 5, 6, and 7 Å, for $[Na@C_{60}]^+$, C_{60}, and $[F@C_{60}]^-$. Data taken from Table 3.

Table 3. Charge Q Enclosed within the Icosahedral Surfaces, Traced Inside and Outside the C_{60} cage and Concentric to It, Calculated at the MPWB1K/3-21+G and MPWB1K/6-31+G* //MPWB1K/6-31+G* Levels[a]

	Q (au)							
	C_{60}		$[F@C_{60}]^-$		$[Na@C_{60}]^+$		$He@C_{60}$	
Surface with d_h, d_p (Å)	3-21+G	6-31+G*	3-21+G	6-31+G*	3-21+G	6-31+G*	3-21+G	6-31+G*
2, 2.0442	−0.8	−0.7	−1.6	−1.5	0.2	0.4	−0.8	−0.7
5, 5.1106	1.2	1.3	0.6	0.7	2.1	2.2	1.2	1.4
6, 6.1327	0.1	0.1	−0.7	−0.9	1.1	1.1	0.1	0.1
7, 7.1548	0.0	0.0	−0.8	−1.0	1.0	1.0	0.0	0.0
10, 10.2212	0.0	0.0	−1.0	−1.0	1.0	1.0	0.0	0.0

[a] d_h (d_p) is the distance of the centers of hexagons (pentagons), belonging to the five surfaces, to O, the center of the complex.

Table 4. Charge Q Enclosed within the Icosahedral Surfaces, Traced Inside and Outside the C_{60} Cage and Concentric to It, Calculated at the MP2/3-21+G//MPWB1K/3-21+G and MP2/6-31+G* //MPWB1K/3-21+G Levels[a]

	Q (au)							
	C_{60}		$[F@C_{60}]^-$		$[Na@C_{60}]^+$		$He@C_{60}$	
Surface with d_h, d_p (Å)	3-21+G	6-31+G*	3-21+G	*6-31+G**	3-21+G	*6-31+G**	3-21+G	6-31+G*
2, 2.0442	−0.9	−0.8	−1.6	−1.5	0.2	0.4	−0.8	−0.8
5, 5.1106	1.3	1.5	0.8	1.0	2.2	2.4	1.4	1.4
6, 6.1327	0.1	0.1	−0.9	−1.0	1.1	1.1	0.1	0.1
7, 7.1548	0.0	0.0	−1.0	−1.0	1.0	1.0	0.0	0.0

[a] d_h (d_p) is the distance of the centers of hexagons (pentagons), belonging to the five surfaces, to O, the center of the complex.

The charges, such as those shown in Table 3, were also calculated for the MP2 electron density. The results are shown in Table 4.

Comparison of results obtained with both basis sets proves that the calculations are characterized by good robustness properties. The results in Tables 3 and 4 indicate that the electron density distributions for C_{60} and $He@C_{60}$ calculated using the 6-31+G* basis are practically the same. The center of the "empty" fullerene cage is not empty: a small negative charge of −0.7 ÷ −0.8 e was found within the first icosahedral surface. According to a simplified view of the electron transfer only between atoms (e.g., He and C), the same positive charge should be located at carbon atoms. In this case, in the space beyond the cage, the density of charge should be null. However it appeared that within the surface characterized by d_h = 5 Å, a charge of 1.5 e is enclosed. Only within the surface of d_h = 7 Å is the total charge null. For ionic fullerenes, within the surface of d_h = 6 Å, the charge is −0.9 or 1.1 e (MPWB1K/6-31+G*) or −1 or 1.1 (MP2/6-31+G*). The expected charge of −1 (for $[F@C_{60}]^-$) or +1 (for $[Na@C_{60}]^+$) is found only at 7 Å.

The results in Tables 3 and 4 suggest that the electric field calculations have also very good robustness properties toward the calculation level.

Table 3 and the right panel of Figure 2 compare the charges found within subsequent icosahedral surfaces characterized by different values of d_h (and d_p). The right panel of Figure 2 shows that the charge distribution in space for C_{60} and its endohedral complexes $[F@C_{60}]^-$ and $[Na@C_{60}]^+$ is similar in shape but characterized by different values of the enclosed charge. Within the smallest surface, the charge may be taken as an approximation of the charge of an atom positioned in the center of the cage. In the case of F as a dopant, its negative charge is greater than −1; this result indicates that F bears not only the additional electron of the system, but there is also some electron density transfer (−0.5 e) from the cage to F^-. In the case of the $[Na@C_{60}]^+$ complex, the Na atom bears a charge of 0.4 e, as if the cage also delivered some electron

dx.doi.org/10.1021/ci300001h | J. Chem. Inf. Model. 2012, 52, 1193−1198

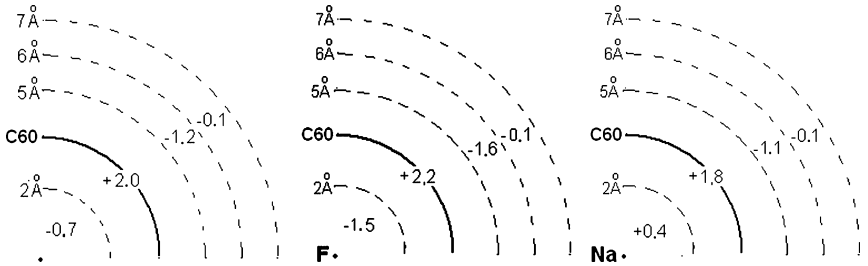

Figure 3. A charge enclosed between concentric icosahedral surfaces drawn inside and outside the fullerene cage and centered at O, for C_{60}, $[F@C_{60}]^-$, and $[Na@C_{60}]^+$. The values in Å denote distances d_h from O to the centers of the hexagons for a given surface; all values of d_h are the same. The full line represents the surface of the C_{60} cage.

density (0.6 e) to the Na^+ atom inside it. The result for the complex with F is at variance with all the data displayed in Table 1. However, for the complex with Na^+, the result is in accordance (this may be accidental) with that generated by the Hirshfeld algorithm (Table 2).

The distribution of electron density can also be depicted as a charge enclosed between concentric surfaces, as shown in Figure 3. In the figure, the broken lines represent fragments of the truncated icosahedral surfaces, centered at O. Figures 2 and 3 show that the field outside the empty fullerene vanishes only at a distance of about 7 Å (this is also true for $He@C_{60}$). For the charged complexes, the expected total charge (−1 e or +1 e) is also found at that distance only.

■ CONCLUSIONS

The spatial distribution of charges in fullerene complexes has been determined for the complexes possessing Ih symmetry with a dopant in the center of the C_{60} cage. The distribution showed that in every case (neutral, cationic, or anionic complexes) a shell extending from 2 to 5 Å, including the carbon atoms inside, bears a charge of about +2 e. Taking the charge enclosed within a sphere with a radius equal 2 Å around the central doping atom as an estimation of the dopant partial charge, we found that the charge on the F dopant equals about −1.5 e, and for Na dopant about 0.4 e. For an He atom inside the cage and for empty C_{60}, the charge confined within the 2 Å sphere was −0.7 e at the MPWB1K or −0.8 e at the MP2 level. This finding points to a flow of negative electron density from the cage to its center. The total charge of the complex, be it 0, +1, or −1, can only be found within a surface distanced about 7 Å from the fullerene center.

■ AUTHOR INFORMATION

Corresponding Author

*E-mail: sadlej@il.waw.pl.

Notes

The authors declare no competing financial interest.

■ ACKNOWLEDGMENTS

We acknowledge the computing grant G44-18 from the Interdisciplinary Center for Mathematical and Computer Modelling (ICM) of the Warsaw University.

We also think Dr. Douglas J. Fox from Gaussian Inc. for his extremely helpful assistance.

■ REFERENCES

(1) Saunders, M.; Jiménez-Vázquez, H. A.; Cross, R. J.; Poreda, R. J. Stable compounds of Helium and Neon:He@C_{60} and Ne@C_{60}. *Science* **1993**, *259*, 1428−1430.

(2) Saunders, M.; Cross, R. J.; Jiménez-Vázquez, H. A.; Shimsi, R.; Khong, A. Noble gas atoms inside fullerenes. *Science* **1996**, *271*, 1693−1697.

(3) Stanisky, C. M.; Cross, R. J.; Saunders, M. Putting Atoms and Molecules into Chemically Opened Fullerenes. *J. Am. Chem. Soc.* **2009**, *131*, 3392−3395.

(4) Wang, Z.-Y.; Su, K.-H.; Yao, X.-P.; Li, Y.-L.; Wang, F. Mechanical and electronic properties of endofullerene Ar@C_{60} studied via structure distortions. *Mater. Chem. Phys.* **2010**, *119*, 406−417.

(5) Pietzak, P.; Weiblinger, M.; Almeida Murphy, T.; Weidinger, A.; Höhne, M.; Dietel, E.; Hirsh, A. Buckminsterfullerene C_{60}: A chemical Faraday cage for atomic nitrogen. *Chem. Phys. Lett.* **1994**, *279*, 259−263.

(6) Weidinger, A.; Waiblinger, M.; Pietzak, B.; Almeida Murphy, T. Atomic nitrogen in C_{60}: N@C_{60}. *Appl. Phys. A: Mater. Sci. Process.* **1998**, *66*, 287−292.

(7) Guha, S.; Nakamoto, K. Electronic structures and spectral properties of endohedral fullerenes. *Coord. Chem. Rev.* **2005**, *249*, 1111−1132.

(8) Liu, S.; Sun, S. Recent progress in the studies of endohedral metallofullerenes. *J. Organomet. Chem.* **2000**, *599*, 74−86.

(9) Rubin, Y.; Jarrosson, T.; Wang, G.-W.; Bartberger, M. D.; Houk, K. N.; Schick, G.; Saunders, M.; Cross, R. J. Insertion of helium and molecular hydrogen through the orifice of an open fullerene. *Angew. Chem., Int. Ed.* **2001**, *40*, 1543−1456.

(10) Komatsu, K.; Murata, M.; Murata, Y. Encapsulation of molecular hydrogen in fullerene C_{60} by organic synthesis. *Science* **2005**, *307*, 238−240.

(11) Kurotobi, K.; Murata, Y. A single molecule of water encapsulated in fullerene C_{60}. *Science* **2011**, *333*, 613−616.

(12) Hesselmann, A.; Korona, T. On the accuracy of DFT-SAPT, MP2, SCS-MP2, MP2C, and DFT+Disp methods for the interaction energies of endohedral complexes of the C_{60} fullerene with a rare gas atom. *Phys. Chem. Chem. Phys.* **2011**, *13*, 732−743.

(13) Jantoljak, H.; Krawez, N.; Loa, I.; Tellgmann, R.; Campbell, E. E. B.; Litvinchuk, A. P.; Thomsen, C. A vibrational spectroscopic study of endohedral Li@C_{60} fullerenes. *Z. phys. Chem. (Muenchen, Ger.)* **1997**, *200*, 157−164.

(14) Slanina, Z.; Uhlík, F.; Lee, S.-L.; Adamowicz, L.; Nagase, S. MPWB1K calculations of stepwise encapsulations: Li_x@C_{60}. *Chem. Phys. Lett.* **2008**, *463*, 121−123.

(15) Ravinder, P.; Subramanian, V. Studies on the encapsulation of various anions in different fullerens using density functional theory calculations and Born-Oppenheimer molecular dynamics simulation. *J. Phys. Chem. A* **2011**, *115*, 11723−11733.

(16) Andreoni, W.; Curioni, A. Ab initio approach to the structure and dynamics of metallofullerens. *Appl. Phys. A: Mater. Sci. Process.* **1998**, *66*, 299−306.

(17) Jin, L.; Zhang, M.; Su, Z.; Shi, L. J. Theoretical study on endohedral complexes C_2H_2-C_{60}, C_2H_4-C_{60}, and C_2H_6-C_{60}. *J. Theor. Comput. Chem.* **2008**, *7*, 1−11.

(18) Ramachandran, C. N.; Sathyamurthy, N. Water clusters in a confined nonpolar environment. *Chem. Phys. Lett.* **2005**, *410*, 348−351.

(19) Greer, J. C. The atomic nature of endohedrally encapsulated nitrogen N@C_{60} studied by density functional and Hartree-Fock methods. *Chem. Phys. Lett.* **2000**, *326*, 567−572.
(20) Cioslowski, J. Endohedral chemistry: Electronic structures of molecules trapped inside the C_{60} cage. *J. Am. Chem. Soc.* **1991**, *113*, 4139−4141.
(21) Krapp, A.; Frenking, G. Is this a chemical bond? A theoretical study of Ng_2@C_{60} (Ng=He, Ne, Ar, Kr, Xe). *Chem.—Eur. J.* **2007**, *13*, 8256−8270.
(22) Pavanello, M.; Jalbout, A. F.; Trzaskowski, B.; Adamowicz, L. Fullerene as an electron buffer: Charge transfer in Li@C_{60}. *Chem. Phys. Lett.* **2007**, *442*, 339−343.
(23) Cramer, C. J. *Essentials of Computational Chemistry*. John Wiley&Sons Ltd., England, 2003, p 279.
(24) Purcell, E. M. *Electricity and Magnetism. Berkeley Physics Course*, McGraw-Hill, Inc. Book Company, New York, 1985, Vol 2, pp 22−25.
(25) Adamo, C.; Barone, V. Exchange functionals with improved long-range behavior and adiabatic connection method without adjustable parameters: The mPW and mPW1PW models. *J. Chem. Phys.* **1998**, *108*, 664−675.
(26) Zhao, Y.; Truhlar, D. G. Hybrid meta density functional theory methods for thermochemistry, thermochemical kinetics, and noncovalent interactions: the MPW1P95 and MPWB1K model and comparative assessment for hydrogen bonding and van der Waals interactions. *J. Phys. Chem. A* **2004**, *108*, 6908−6918.
(27) Frisch, M. J.; Trucks, G. W.; Schlegel, H. B.; Scuseria, G. E.; Robb, M. A.; Cheeseman, J. R.; Scalmani, G.; Barone, V.; Menucci, G. A.; Petersson, H.; Nakatsuji, H.; Caricato, M.; Li, X,; Hratchian, H. P.; Izmaylov, A. F.; Bloino, J.; Zheng, G.; Sonnenberg, J. L.; Hada, M.; Ehara, M.; Toyota, K.; Fukuda, R.; Hasegawa, J.; Ishida, M.; Nakajima, T.; Honda, Y.; Kitao, O.; Nakai, H.; Vreven, T.; Montgomery Jr. J. A.; Peralta, J. E.; Ogliaro, F.; Bearpark, M.; Heyd, J. J.; Brothers, E.; Kudin, K. N.; Staroverov, V. N.; Kobayashi, R.; Normand, J.; Raghavachari, K.; Rendell, A.; Burant, J. C.; Iyengar, S. S.; Tomasi, J.; Cossi, M.; Rega, N.; Millam, J. M.; Klene, M.; Knox, J. E.; Cross, J. B.; Bakken, V.; Adamo, C.; Jaramillo, J.; Gomperts, R.; Stratmann, R. E.; Yazyev, O.; Austin, A. J.; Cammi, R.; Pomelli, C.; Ochterski, J. W.; Martin, R. L.; Morokuma, K.; Zakrzewski, V. G.; Voth, G. A.; Salvador, P.; Danneneberg, J. J.; Dapprich, S.; Daniels, A. D.; Farkas, O.; Foresman, J. B.; Ortiz, J. V.; Cioslowski, J.; Fox, J. D.; Gaussian 09, Revision B.01; Gaussian Inc.; Wallingford CT, 2009.
(28) Hehre, W. J.; Radom, L.; v.R.Schleyer, P.; Pople, J. A. *Ab Initio Molecular Orbital Theory*. John Wiley@Sons, New York, 1986, pp 71−88.
(29) Mulliken, R. S. Electronic population analysis on LCAO-MO molecular wave functions. I. *J. Chem. Phys.* **1955**, *23*, 1833−1840.
(30) Reed, A. E.; Curtiss, L. A.; Weinhold, F. Intermolecular interactions from a natural bond orbital, donor-acceptor view-point. *Chem. Rev.* **1988**, *88*, 899−926.
(31) Löwdin, P.-O. On the orthogonality problem. *Adv. Quantum Chem.* **1970**, *5*, 185−199.
(32) Bader, R. W. F. A quantum theory of molecular structure and its applications. *Chem. Rev.* **1991**, *91*, 893−928.
(33) Hirshfeld, F. L. Bonded-atom fragments for describing molecular charge densities. *Theor. Chim. Acta* **1977**, *44*, 129−138.
(34) Breneman, C. M.; Wiberg, K. B. Determining atom-centered monopoles from molecular electrostatic potentials. The need for high sampling density in formamide conformational analysis. *J. Comput. Chem.* **1990**, *11*, 361−373.
(35) Besler, B. H.; Merz, K. M., Jr.; Kollman, P. A. Atomic charges derived from semiempirical methods. *J. Comput. Chem.* **1990**, *11*, 431−439.
(36) *AIM 2000* Version 2.0, Biegler König F.; Schönbohm J., 2002. http://www.aim2000.de (accessed January 01, 2002; last changes April 02, 2009).
(37) Weisstein, E. W. *Line*. From MathWorld − A Wolfram Web Resource. http://mathworld.wolfram.com/Line.html (last updated February 29, 2012).
(38) Frisch, Æ.; Frisch, M. J.; Trucks, G. W. *Gaussian 03 User's Reference*, Gaussian, Inc.: Carnegie, PA 15106 USA, 2003, p 67.
(39) Purcell, E. M. *Electricity and Magnetism. Berkeley Physics Course*, McGraw-Hill, Inc. Book Company, New York, 1985, Vol. 2, pp 8, 475.